

Dynamical freeze-out in event-by-event hydrodynamics

Hannu Holopainen¹ and Pasi Huovinen²

¹ Frankfurt Institute for Advanced Studies, Ruth-Moufang-Str. 1, D-60438 Frankfurt am Main, Germany,

² Institut für Theoretische Physik, Johann Wolfgang Goethe-Universität, Max-von-Laue-Str. 1, 60438 Frankfurt am Main, Germany

E-mail: holopainen@fias.uni-frankfurt.de

Abstract. In hydrodynamical modeling of the ultrarelativistic heavy-ion collisions the freeze-out is typically performed at a constant temperature or density. In this work we apply a dynamical freeze-out criterion, which compares the hydrodynamical expansion rate with the pion scattering rate. Recently many calculations have been done using event-by-event hydrodynamics where the initial density profile fluctuates from event to event. In these event-by-event calculations the expansion rate fluctuates strongly as well, and thus it is interesting to check how the dynamical freeze-out changes hadron distributions with respect to the constant temperature freeze-out. We present hadron spectra and elliptic flow calculated using (2+1)-dimensional ideal hydrodynamics, and show the differences between constant temperature and dynamical freeze-out criteria. We find that the differences caused by different freeze-out criteria are small in all studied cases.

1. Introduction

In hydrodynamical modeling of heavy-ion collisions the freeze-out is typically assumed to take place instantaneously on a very thin hypersurface of constant temperature or energy density, and the fluid is converted to particles using the Cooper-Frye formula. However, from microscopic point of view the system should freeze-out either when the mean free path of particles is larger than the system size, or when the expansion rate exceeds the scattering rate of particles [1]. Neither of these criteria is directly proportional to temperature nor density. The dynamical freeze-out criterion which directly compares scattering rate with the hydrodynamical expansion rate was applied to hydrodynamical modeling already some time ago [2], but it has not been widely used.

Earlier studies with smooth optical Glauber initial profiles have shown that while the freeze-out surface from the dynamical condition differ significantly from the constant temperature surface, the effect on observable particle spectra is small [3]. However, no studies of the effect on elliptic flow have been done yet. As well, event-by-event hydrodynamical calculations have become popular recently, and in such a case the flow develops more violently than when averaged initial state is used. Thus it is not obvious whether the difference between the two freeze-out conditions is small also when the initial density fluctuates event-by-event.

The problem of freeze-out is not fully resolved in the hybrid models either. In these models the hydrodynamical evolution is stopped while the hadrons are still interacting, the fluid is

converted to individual hadrons, and the subsequent evolution of hadrons is described using a hadron cascade [4]. The switch from fluid to cascade is usually done on a constant temperature hypersurface, but the final results depend on the temperature where the switch is done [5, 6, 7]. It is possible that switching on a constant Knudsen number instead would lead to results which are less sensitive to the actual value of the switching parameter.

In this proceedings we compare the dynamical freeze-out criterion with the constant temperature one. We start by introducing our hydrodynamical model and the dynamical freeze-out criterion. We compare the properties of the freeze-out surfaces obtained using different freeze-out criteria and averaged initial state, and calculate the particle p_T -spectra and elliptic flow in these cases. Finally we apply the two different criteria to an event-by-event calculation, study the surfaces, and calculate the particle p_T -spectra and elliptic flow.

2. Hydrodynamical model

Here we use a slightly modified version of the ideal event-by-event hydrodynamics framework presented in [8]. We solve the ideal hydrodynamical equations

$$\partial_\mu T^{\mu\nu} = 0 \quad \partial_\mu N^\mu = 0, \quad (1)$$

where $T^{\mu\nu}$ is the ideal energy-momentum tensor and N^μ is the net-baryon number current. We assume longitudinal boost invariance and thus the numerical problem reduces to (2+1)-dimensions. In order to close the set of equations we need an equation of state (EoS) and our choice here is s95p-v1 from Ref. [9].

Particle emission from the freeze-out surface is calculated using conventional Cooper-Frye formula

$$\frac{dN}{d^2p_T dy} = \int_\Sigma f(x, p) p^\mu d\Sigma_\mu, \quad (2)$$

where we integrate over the freeze-out surface Σ , $f(x, p)$ is particle distribution and p^μ is the four momentum of the emitted particle. The freeze-out surface elements $d\Sigma_\mu$ are found with CORNELIUS++¹ using the algorithm described in [7].

After the thermal particle spectra are calculated using Cooper-Frye, we sample particles using these spectra as a probability distributions. Sampling is done as described in [8]. Thus the number of each particle species is fixed, but the total energy of particles in each event can fluctuate. Then the strong and electromagnetic decays are done one particle at a time. In [8] decays were done using PYTHIA, which meant that all hadron resonances included in the EoS could not be used. Here we use a separate decay program, which makes it possible to include all hadrons present in the EoS.

In this contribution we consider Au+Au collisions at Relativistic Heavy Ion Collider (RHIC) with $\sqrt{s_{NN}} = 200$ GeV. Smooth initial conditions for the entropy density are obtained from the optical Glauber model using a mixture of binary (75%) and wounded nucleon (25%) profiles. For the fluctuating initial conditions a Monte Carlo Glauber model with same mixture is used. Monte Carlo Glauber model gives only the positions of the wounded nucleons and binary collisions and we need to distribute entropy around these positions before we can initialize hydrodynamical evolution. Our choice is a 2-dimensional Gaussian:

$$s(x, y) = \text{const.} \sum_{\text{wn, bc}} \frac{1}{2\pi\sigma^2} \exp \left[-\frac{(x - x_i)^2 + (y - y_i)^2}{2\sigma^2} \right], \quad (3)$$

¹ CORNELIUS surface finding subroutine is available at the OSCAR code repository, <https://karman.physics.purdue.edu/OSCAR/>.

where σ is a free parameter controlling the width of the Gaussian. Typical values for this fluctuation size parameter is order of 0.5 fm, our choices here are 0.4 fm and 0.8 fm. For net-baryon density a pure wounded nucleon profile is used in both cases. We choose the initial time to be $\tau_0 = 0.6$ fm.

Because there are differences between the two Glauber models and the mixtures are not defined exactly in the same way, we cannot compare the results obtained with smooth and fluctuating initial conditions. Here we concentrate on the effects coming from the freeze-out condition and comparisons between smooth and fluctuating initial conditions with constant temperature freeze-out can be found *e.g.* from Ref. [8].

3. Dynamical freeze-out condition

For the system to maintain kinetic equilibrium, the scattering rate should be much larger than the expansion rate. In other words

$$K = \frac{\theta}{\Gamma} \ll 1, \quad (4)$$

where Γ is the scattering rate and θ is the hydrodynamical expansion rate. As a ratio of (an inverse of) a macroscopic length scale to (an inverse of) a microscopic length scale, the ratio K can be identified as a Knudsen number — which must be larger than one for hydrodynamics to be valid as well. Since we are interested in freeze-out, the region of last rescattering, we replace the vague requirement $K \ll 1$ by assuming that the system is reasonably close to equilibrium until $K = K_{\text{fo}} = 1$, and test the sensitivity of the spectra to the exact value of K_{fo} by using values $K_{\text{fo}} = 0.5 - 2$.² Our initial assumption $K_{\text{fo}} = 1$ is a posteriori justified by a good reproduction of the measured particle spectra. When we compare to results calculated using freeze-out at constant temperature, we use $T_{\text{fo}} = 140$ MeV for the same reason.

The expansion rate of a system is given by the hydrodynamical model. For a boost-invariant system it is evaluated as

$$\theta = \partial_\mu u^\mu = \partial_\tau u^\tau + \partial_x u^x + \partial_y u^y + u^\tau / \tau. \quad (5)$$

We evaluate the scattering rate of pions in kinetically (but not necessarily chemically) equilibrated hadron-resonance gas as

$$\Gamma = \frac{1}{n_\pi(T, \mu_\pi)} \sum_i \int d^3 p_\pi d^3 p_i f_\pi(T, \mu_\pi) f_i(T, \mu_i) \frac{\sqrt{(s - s_a)(s - s_b)}}{2E_\pi E_i} \sigma_{\pi i}(s), \quad (6)$$

where n_π is the density of pions, $f_i(T, \mu_i)$ is the thermal distribution function, $\sqrt{(s - s_a)(s - s_b)}/(2E_\pi E_i)$ is the relative velocity, $\sigma_{\pi i}$ is the cross section for scattering of pion with particle i , and the summation over i runs over all particle species included in the EoS. Cross sections are evaluated as in the UrQMD model [10], *i.e.* the main contribution comes from resonance formation which is evaluated using the relativistic Breit-Wigner formula. Details of this calculation will be published in a later paper.

Scattering rates are different for different particle species, and thus one could argue that freeze-out should take place when the scattering rate of a particular species is equal to the expansion rate, which would mean freeze-out at different times for different particle species. However, to be consistent, this approach would require us to modify fluid dynamics in such a way that when *e.g.* pions are decoupled, they are removed from the fluid. For the subsequent evolution of the remaining fluid we should then include the interactions with the non-equilibrated pion cloud, which is clearly beyond the capabilities of fluid dynamics. Thus we make the

² In Ref. [2] it was argued that $K_{\text{fo}} = 2$ would give the region of the last rescattering.

simplifying approximation that all the particle species decouple at the same time, and since the pions are the most abundant particles, we base our freeze-out description on the scattering rate of pions.

4. Results with smooth initial conditions

We start by studying the freeze-out systematics with smooth initial conditions. First in Fig. 1 we compare the freeze-out surfaces with both the constant temperature and the dynamical freeze-out criteria. We can see that with the dynamical condition the edges of the system decouple earlier and the center of the system lives little longer. This is because near the edges the pressure gradients are large and thus the expansion rate is large. In the center of the system the expansion is not so rapid and thus the center can maintain the kinetical equilibrium at lower temperatures, *i.e.* at smaller scattering rates.

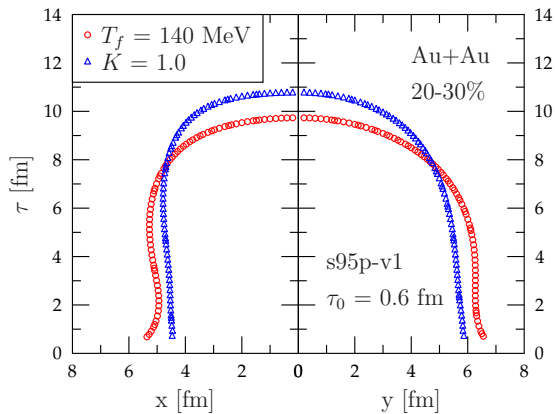


Figure 1. Freeze-out surface along positive x - and y -axis in 20-30% central Au+Au collisions at $\sqrt{s_{NN}} = 200$ GeV. Surfaces are shown with both dynamical and constant temperature criterion.

In Fig. 2 we plot the temperature on the freeze-out surfaces with both conditions. Naturally with the constant temperature criterion the curve is constant, but with the dynamical freeze-out the temperature can vary a lot. As already explained above, the edges decouple earlier with the dynamical conditions and thus the edges are hotter than in the constant temperature case. Accordingly, the center the system is little bit cooler with the dynamical freeze-out.

The radial velocity on the surface along the x -axis as a function of time is plotted in Fig. 3. Since with the dynamical condition the edges decouple earlier, the largest flow velocities are cut away as we can see in the figure. For the high- p_T ($\gtrsim 1$ GeV) emission the part of the surface where the flow velocity is largest is most important and one could expect that the two different freeze-out conditions could give different results. However, the effect of smaller transverse flow is countered by the larger temperature and thus it is difficult to say what happens based on these figures alone.

It is interesting to see how the freeze-out surface changes when we change the freeze-out condition, but the experiments cannot measure the properties of the freeze-out surface itself, but rather the particle spectra and its anisotropies. In Fig. 4 we have plotted the spectra of positively charged pions and protons. We see that results from different freeze-out conditions are basically on top of each other. This indicates that the increased temperature at the edges cancels the effect of reducing the maximum flow velocity.

We also plot the elliptic flow of charged hadrons in Fig. 5 with respect to the reaction plane (defined by impact parameter and beam axis). Also here the freeze-out criterion does not play a role and the result is the same with both conditions. From the particle spectra and elliptic flow we can conclude that the constant temperature freeze-out gives the same answers as dynamical freeze-out despite the fact that the surface itself shows some sensitivity to the criterion.

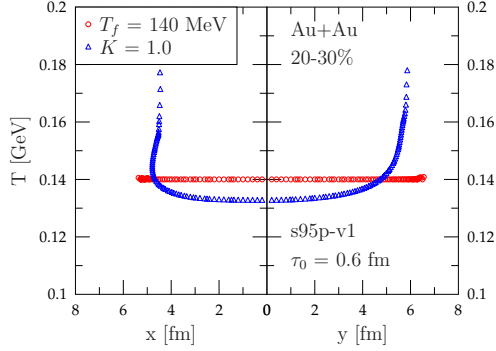


Figure 2. Temperature on the freeze-out surface along positive x - and y -axis in 20-30% central Au+Au collisions at $\sqrt{s_{NN}} = 200$ GeV. Surfaces are shown with both dynamical and constant temperature criterion.

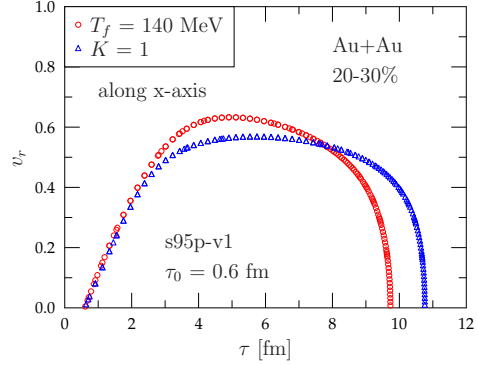


Figure 3. Radial velocity on the freeze-out surface along positive x - and y -axis in 20-30% central Au+Au collisions at $\sqrt{s_{NN}} = 200$ GeV. Surfaces are shown with both dynamical and constant temperature criteria.

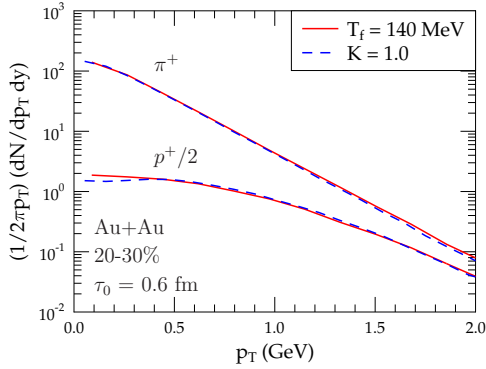


Figure 4. Spectra of positively charged pions and protons in 20-30% central Au+Au collisions at $\sqrt{s_{NN}} = 200$ GeV. Results are shown with both dynamical and constant temperature criterion.

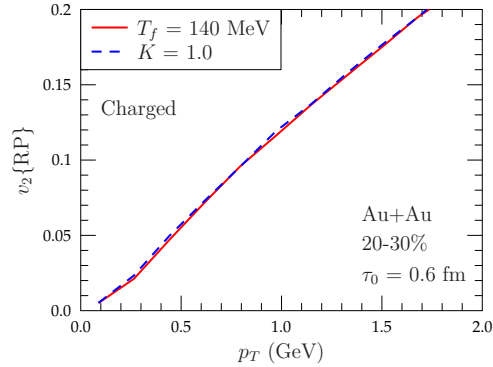


Figure 5. Elliptic flow of charged particles calculated with event plane method in 20-30% central Au+Au collisions at $\sqrt{s_{NN}} = 200$ GeV. Results are shown with both dynamical and constant temperature criterion.

Finally, we show how the results depend on the freeze-out parameter K_{fo} . In Fig. 6 we plot the freeze-out surfaces with $K_{fo} = 0.5, 1.0$ and 2.0 and in Fig. 7 we show the p_T -spectra of pions and protons with these three values. We see that with larger value of K_{fo} the system lives longer. This naturally leads to the fact that more flow is developed and thus the spectra for pions and protons is flatter. Also because we have chemical equilibrium until freeze-out, the number of protons depends on the freeze-out value K since the average temperature on the surface depends on K . Introducing a separate chemical freeze-out would solve this problem and this will be done in the future.

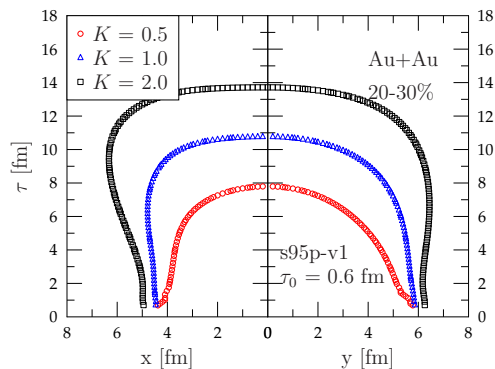


Figure 6. Freeze-out surface along positive x - and y -axis in 20-30% central Au+Au collisions at $\sqrt{s_{NN}} = 200$ GeV. Results are shown with three different freeze-out parameter values.

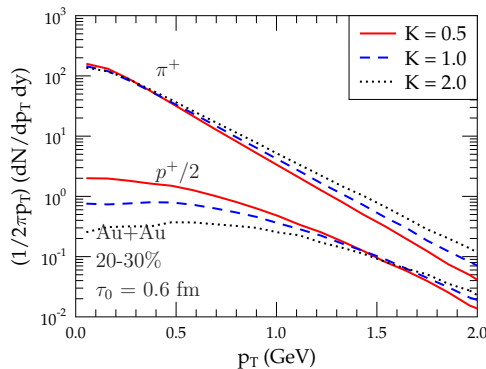


Figure 7. Spectra of positively charged pions and protons in 20-30% central Au+Au collisions at $\sqrt{s_{NN}} = 200$ GeV. Results are shown with three different freeze-out parameter values.

5. Results with fluctuating initial conditions

In the previous section we saw that the particle spectra and elliptic flow do not change when we switch from constant temperature freeze-out to the dynamical one. However, we used smooth initial conditions, where the expansion rate behaves smoothly. When we include event-by-event density fluctuations to the initial state, the flow develops more violently and the freeze-out criterion could affect the final spectra.

In the first calculations we used a quite small smearing parameter $\sigma = 0.4$ fm, which means that there is a lot of structure in the initial energy density distribution. Consequently the expansion rate can vary a lot during the evolution. An example of the freeze-out surface with dynamical condition is shown in Fig. 8. We can see that many long living small scale structures exist: Thin rod-like “horns” and narrow but wide “fins”. Conceptually this kind of structures are difficult, since their size is smaller than the average mean free path of particles, and thus from microscopic point of view, they shouldn’t exist.

The same event with double the smearing parameter is shown in Fig. 9, and we immediately notice that the surface is much smoother and only one fin remains. Thus before studying the effects of the fins and horns, one can use smoother initial states to check if the freeze-out condition is more important when the fluctuating initial state is used than when an averaged initial state is used. More advanced studies where the effect of the fins and horns are explored are left for future work.

The reason for the fin and horn formation is that with fluctuations there are some regions where the expansion rate goes to negative, *i.e.* there is compression. By definition the dynamical freeze-out condition does not allow those regions to freeze-out, no matter how long living or cold they are. It is obvious that the smaller the smearing parameter σ , the more pronounced the initial peaks and valleys are in the initial density profile, and the more common the regions are where the fluid compresses instead of expanding. Thus the freeze-out surface is much more complicated in Fig. 8 than in Fig. 9.

In Fig. 10 we plot the spectra of pions and protons and in Fig. 11 we plot the elliptic flow of charged hadrons. Here v_2 is calculated with event plane method in the same way as in Ref. [8]. We can see that also in this situation there are no differences between the two freeze-out conditions. The situation is similar with and without initial state fluctuations, although the

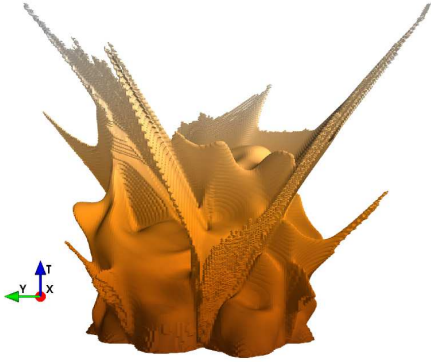


Figure 8. Freeze-out surface with fluctuating initial conditions with $\sigma = 0.4$ fm.

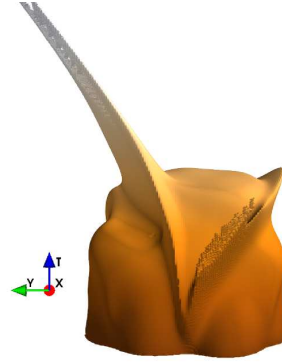


Figure 9. Freeze-out surface with fluctuating initial conditions with $\sigma = 0.8$ fm.

reason for this may be that we had to use very smooth event-by-event initial states in order to get rid of the multiple fins and horns, which we consider unphysical.

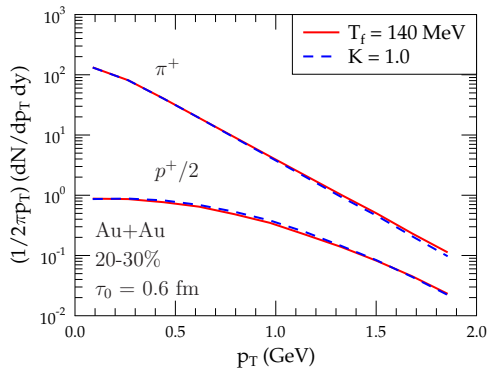


Figure 10. Spectra of positively charged pions and protons in 20-30% central Au+Au collisions at $\sqrt{s_{NN}} = 200$ GeV. Results are shown with both dynamical and constant temperature criterion.

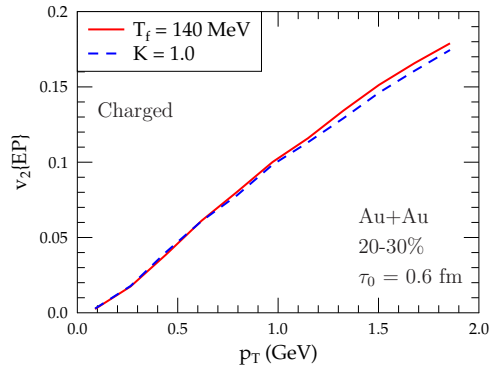


Figure 11. Elliptic flow of charged particles calculated with event plane method in 20-30% central Au+Au collisions at $\sqrt{s_{NN}} = 200$ GeV. Results are shown with both dynamical and constant temperature criterion.

6. Conclusions

We have argued that the constant temperature freeze-out is an oversimplification, but the differences compared to the dynamical freeze-out criterion are small in particle spectra and elliptic flow. Freeze-out surfaces itself are different, but effects from the increased temperature and decreased radial flow at the edges in dynamical freeze-out cancel each other and finally there are no visible effects in the particle spectra and elliptic flow.

However, here our event-by-event studies were limited to the case where initial fluctuation smearing parameter was large. Because of that our initial states are very smooth and we can expect that the behavior is very similar to the optical Glauber model case. With smaller smearing parameters the freeze-out surface had many small scale structures (which we called horns and

fins) which are most probably unphysical. Thus we did not evaluate the particle distributions yet in that case. Ultimately one needs to evaluate the spectra in this case too, but before that we have to devise a way to distinguish the effect of these small scale structures on the spectra to know when the change in the spectra might be unphysical.

On the other hand it has been shown that finite viscosity smoothens the density distribution at the end of the evolution considerably [11]. Thus the small scale structures may disappear altogether in a viscous calculation, and it would be interesting and easier to apply dynamical freeze-out criterion in the context of viscous hydrodynamics.

The work of H.H. was supported by the Extreme Matter Institute (EMMI) and the work of P.H. by BMBF under contract no. 06FY9092.

References

- [1] Bondorf J P, Garpman S I A and Zimanyi J 1978 *Nucl. Phys. A* **296** 320
- [2] Hung C M and Shuryak E V 1998 *Phys. Rev. C* **57** 1891
- [3] Eskola K J, Niemi H and Ruuskanen P V 2008 *Phys. Rev. C* **77** 044907
- [4] Petersen H, Steinheimer J, Baur G, Bleicher M and Stocker H 2008 *Phys. Rev. C* **78** 044901
- [5] Song H, Bass S A and Heinz U 2011 *Phys. Rev. C* **83** 024912
- [6] Hirano T, Huovinen P, Murase K and Nara Y 2012 Integrated Dynamical Approach to Relativistic Heavy Ion Collisions *Preprint* arXiv:1204.5814 [nucl-th]
- [7] Huovinen P and Petersen H 2012 Particlization in hybrid models *Preprint* arXiv:1206.3371 [nucl-th]
- [8] Holopainen H, Niemi H and Eskola K J 2011 *Phys. Rev. C* **83** 034901
- [9] Huovinen P and Petreczky P 2010 *Nucl. Phys. A* **837** 26
- [10] Bass S A *et al.* 1998 *Prog. Part. Nucl. Phys.* **41** 255
- [11] Schenke B, Jeon S and Gale C 2011 *Phys. Rev. Lett.* **106** 042301